

1 **Comments on the paper “Two independent real-time precursors of the 7.8 M earthquake in**  
2 **Ecuador based on radioactive and geodetic processes – Powerful tools for an early warning**  
3 **system” by Toulkeridis et al. (2019)**

4 Hugo Yepes<sup>1\*</sup>, Jean-Mathieu Nocquet<sup>2,3</sup>, Benjamin Bernard<sup>1</sup>, Pablo B. Palacios<sup>1</sup>, Sandro Vaca<sup>1</sup>,  
5 Santiago Aguaiza<sup>1</sup>

6 <sup>1</sup> *Instituto Geofísico – Escuela Politécnica Nacional, Ladrón de Guevara E11-253 y Andalucía,*  
7 *Quito, Ecuador*

8 <sup>2</sup> *Université Côte d’Azur, IRD, CNRS, Observatoire de la Côte d’Azur, Geoazur, Valbonne, F06560,*  
9 *France*

10 <sup>3</sup> *Institut de Physique du Globe de Paris, Université de Paris, UMR 7154, Paris, F75005, France*

11 \* *Corresponding author: [hyepes@igepn.edu.ec](mailto:hyepes@igepn.edu.ec)*

12 This is a preprint submitted to EarthArXiv

13 This article was submitted to Journal of Geodynamics on April 17<sup>th</sup> 2019 (status on June 18<sup>th</sup> 2019:  
14 Accepted)

15 **Abstract**

16 In the paper entitled “Two independent real-time precursors of the 7.8 M earthquake in Ecuador  
17 based on radioactive and geodetic processes – Powerful tools for an early warning system”,  
18 Toulkeridis et al. (2019) claim that they found radiation and GPS signal anomalies before the April  
19 16<sup>th</sup> 2016 Pedernales earthquake (Ecuador) and that their findings can be used to forecast  
20 earthquakes in the medium and short term in active continental margins. Using an extended data set  
21 that overlaps Toulkeridis et al. (2019) study period, we find: (1) the success rate of predicting  
22 earthquakes using radiation anomalies is 2.5%; (2) radiation anomalies, including the one recorded

23 during the hours before the M 7.8 earthquake, temporally correlate with local rainfall; (3)  
24 Toulkeridis et al. (2019) GPS results are physically unrealistic and inconsistent with previously  
25 published GPS and InSAR analysis; (4) there is no anomaly in the GPS time series before the  
26 earthquake. Therefore, Toulkeridis et al. (2019) results are not reliable evidence of precursors to the  
27 M 7.8 earthquake in 2016 in Ecuador, and their proposed method cannot be used to forecast  
28 earthquakes.

## 29 **1. Introduction**

30 After a major earthquake hits populated areas, there are often individuals, either scientists, emer-  
31 gency professionals or laypeople who look for precursory signals that could have been recognized  
32 and communicated prior to the event, thus avoiding the number of deaths and injuries. The 2009  
33 L'Aquila earthquake is one of the most recent and notorious examples for this (Jordan et al, 2011),  
34 and the amateur prediction and its aftermath has the scientific community erring on the right side  
35 (Kolbert, 2015).

36 The scientific literature abounds with success stories about earthquake precursors being retrospec-  
37 tively identified after major earthquakes (Geller, 1997; Uyeda et al. 2009), but only a handful of ex-  
38 amples exist for genuine short-term forecasts such as the M 7.3 earthquake in Haicheng, China, in  
39 1975 (National Research Council, 2003). The search for diagnostic precursors has not yet produced  
40 a successful short-term prediction scheme (Jordan et al. 2011) and any proposed forecast/prediction  
41 methodology must follow a rigorous and transparent process of evaluation (Peresan et al. 2012).

42 In the paper “Two independent real-time precursors of the 7.8 M earthquake in Ecuador based on  
43 radioactive and geodetic processes – Powerful tools for an early warning system” Toulkeridis et al.  
44 (2019) compare gamma radiation time series from a single sensor installed in the Andes at Lasso  
45 (Lat.: S 0.7898°, Long.: W 78.6152°) with the occurrence of earthquakes. They claim that almost all  
46 earthquakes with magnitude  $M \geq 5$ , and located up to 250 km from the sensor, occurred few hours

47 after a significant positive radiation anomaly, including the M 7.8 earthquake on April 16<sup>th</sup> 2016  
48 whose epicenter was about 200 km from the sensor. Toulkeridis et al. (2019) further claim that they  
49 observe a ~1 m transient displacement at all continuous GPS sites in Ecuador several minutes prior  
50 to the M 7.8 earthquake. They indicate that the whole GPS network recorded a northward instanta-  
51 neous displacement exceeding 1 m at most GPS sites at the time of the earthquake. They conclude  
52 that real-time monitoring of radiation and of GPS displacement can be used to implement an early  
53 warning system for forecasting earthquakes in the medium and short terms.

54 Our comment includes the analysis of a 15 month-long radiation time series from the same sensor  
55 as Toulkeridis et al. (2019) that overlaps their study period. We show that the detection performance  
56 of earthquakes is very poor, while correlation with local rainfalls is high, as it is seen during the  
57 hours preceding the M 7.8 earthquake. When analyzing the GPS data, we find no transient  
58 displacement anomaly before the earthquake. We further show that their GPS results are: (1)  
59 inconsistent with the known physics of earthquakes; (2) of bad quality compared with the standard  
60 state-of-the-art of GPS analysis; and (3) inconsistent with independent estimates of displacements  
61 for the Ecuador earthquake.

## 62 **2. Radiation precursors**

### 63 2.1. Method, data availability, operating conditions and detection range

64 We solicited the time series to NOVACERO, the firm owning the Radiation Portal Monitor (RPM)  
65 used by Toulkeridis et al. (2019). We have been given about 15 months of radiation data  
66 overlapping their period of study. The LUDLUM model 4525 RPM used in this work is equipped  
67 with an EJ-200 plastic scintillator that reacts in the presence of gamma radiation and optionally to  
68 neutron emissions. It is designed to detect radioactive material in scrap metal for recycling purposes.  
69 Besides radioactive material, various natural processes can be the source of gamma rays such as  
70 thunderstorms, solar flares and cosmic rays (Marisaldi et al., 2013). Toulkeridis et al. (2019) claim

71 that they detect radiation anomalies associated to earthquakes located up to 250 km away from the  
72 sensor. In Figure 4 of their paper, they show the radiation time series for four earthquakes to support  
73 their hypothesis (also in Figure C1). However, they do not provide neither a systematic statistical  
74 analysis for the whole time series nor a quantitative performance assessment of using radiation time  
75 series for earthquake forecast. Here we present two statistical analyses. The first compares the  
76 gamma radiation anomalies with the earthquake occurrences, and the second highlights a significant  
77 correlation between radiation anomalies and local rainfalls.

## 78 2.2. Gamma radiation anomalies prior to earthquakes

79 Statistical analysis is a must-do process when assessing the potential of seismic precursors (Chen et  
80 al. 2004; Uyeda et al. 2009), where all cases confirming or rejecting the studied hypothesis must be  
81 clearly presented. In order to assess whether radiation anomalies are reliable earthquakes precursors  
82 in Ecuador, we perform a statistical analysis of the temporal correlation between the radiation  
83 anomalies and earthquakes occurrence during the 15-month time window of radiation level  
84 provided by NOVACERO. This time window overlaps the period used in Toulkeridis et al. (2019)  
85 as indicated previously. Following Toulkeridis et al. (2019) method, we selected all earthquakes of  
86 magnitude  $M \geq 5$  from the NEIC catalogue (<https://earthquake.usgs.gov/earthquakes/search/>) in a  
87 250 km radius around the RPM, resulting in a list of 19 earthquakes (Table 1) which includes the  
88 four events, with  $M \geq 5$ , shown in Figure 4 of Toulkeridis et al. (2019).

89 In order to identify the gamma radiation anomalies, we first fill the gaps with median values using  
90 the entire time series. When we find more than one value for the same minute, we take their average.  
91 We filter the time series using a low-pass zero-shift filter, for periods larger than one hour, in order  
92 to identify only hours-long anomalies, as those shown by Toulkeridis et al. (2019). Then, we  
93 normalize this filtered time series with the largest amplitude and compute the square of it to  
94 enhance anomalies. With this final time series (second trace in Figure C2) we define the anomalies  
95 (third trace in Figure C2) as time series periods with amplitudes larger than their 98% percentile.

96 We find 162 anomalies, which includes all those presented in Toulkeridis et al. (2019). As an  
 97 indicator of the temporal variability of the radiation time series, we note that choosing a 95%  
 98 percentile results in 899 anomalies, while using percentiles equal or larger than 99% would not  
 99 include all the anomalies presented in Toulkeridis et al. (2019). Finally, we decide to associate an  
 100 earthquake to a radiation anomaly if the earthquake occurs either during the anomaly or within a 6-  
 101 hour time window after the anomaly's final time. We select these association criteria because, in the  
 102 cases presented by the authors, the earthquakes happen during the anomaly (Fig 4A) or up to three  
 103 hours after the time of the anomaly (Fig. 4B).

104 Table 1. List of the earthquakes  $M \geq 5$  in a 250 km radius around NOVACERO sensor between  
 105 January 2015 and May 2016 (source: <https://earthquake.usgs.gov/earthquakes/search/>)

Date (UTC-05:00)	Latitude	Longitude	Depth (km)	Magnitude (M)
2015-03-27 16:59	-1.201	-77.584	195.0	5.5
2015-04-28 06:19	-2.086	-79.623	89.0	5.4
2015-05-30 01:26	1.220	-79.570	13.0	5.3
2015-10-15 05:07	-2.502	-78.762	97.1	5.4
2016-03-05 19:54	-1.428	-80.401	10.0	5.1
2016-04-16 18:58	0.382	-79.922	20.6	7.8
2016-04-16 19:29	-0.265	-80.464	15.5	5.5
2016-04-17 02:14	-0.385	-80.201	23.9	5.8
2016-04-17 04:23	-0.234	-80.694	10.0	5.6
2016-04-19 17:22	0.578	-80.025	11.0	5.6
2016-04-20 03:33	0.639	-80.210	14.0	6.2
2016-04-20 03:35	0.708	-80.035	10.0	6.0
2016-04-21 22:03	-0.292	-80.504	10.0	6.0
2016-04-21 22:20	-0.281	-80.504	10.3	5.9
2016-04-21 23:31	-0.421	-80.543	10.0	5.0
2016-04-22 20:24	0.613	-80.252	10.0	5.7
2016-04-26 16:58	-0.194	-80.731	10.0	5.4
2016-05-18 02:57	0.426	-79.790	16.0	6.7
2016-05-18 11:46	0.495	-79.616	29.9	6.9

106

107 We only find 4 earthquakes, with magnitude  $M \geq 5$ , being associated with radiation anomalies.  
108 Namely, two of them (M 5.4 on October 15<sup>th</sup> 2015 and M 7.8 on April 16<sup>th</sup> 2016) are shown in the  
109 Figure 4A and 4C of Toulkeridis et al. (2019), whereas the third is a M 5.5 aftershock occurring 30  
110 minutes after the M 7.8 earthquake (Figure C1), which is associated with the same radiation  
111 anomaly, and is not presented by Toulkeridis et al. (2019). The fourth associated earthquake is the  
112 M 5.1, wrongly labeled 5.5M in Toulkeridis et al. (2019), that occurred on March 6<sup>th</sup> 2016 at  
113 00:54:41 UTC. This event is shown after the second anomaly in Figure 4B from Toulkeridis et al.  
114 (2019) but the date on their figure is wrong. Two main flaws appear in Figure 4B: (1) the radiation  
115 time series is presented 24 hours ahead of its actual time: for instance, the first anomaly starts at the  
116 beginning of March 4<sup>th</sup> (at 00:12 Local Time, 05:12 UTC), when it actually occurs on March 5<sup>th</sup> at  
117 05:12 UTC (Figure C1); (2) the earthquake after the first anomaly does not exist, it is actually a M  
118 4.3 earthquake, which occurred on 4 March at 06:25 (Local Time, 11:25 UTC) without any  
119 precursory radiation anomaly (Figure C1).

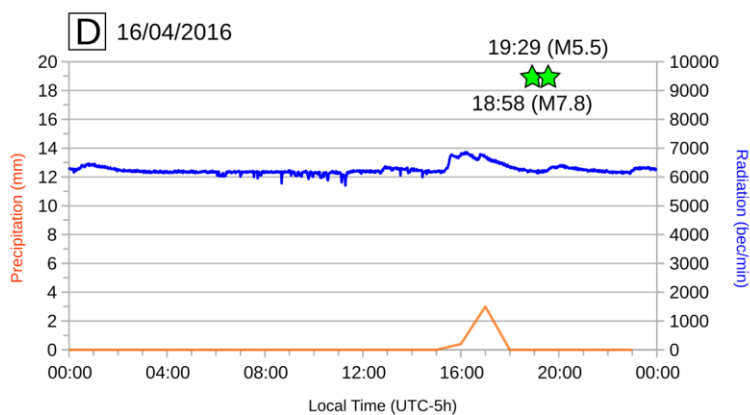
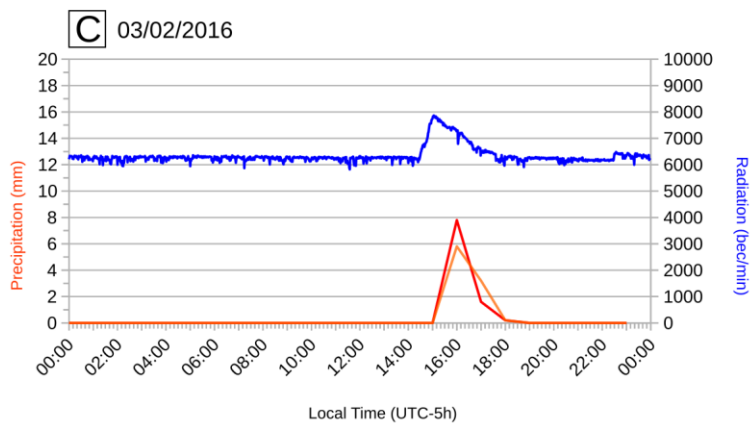
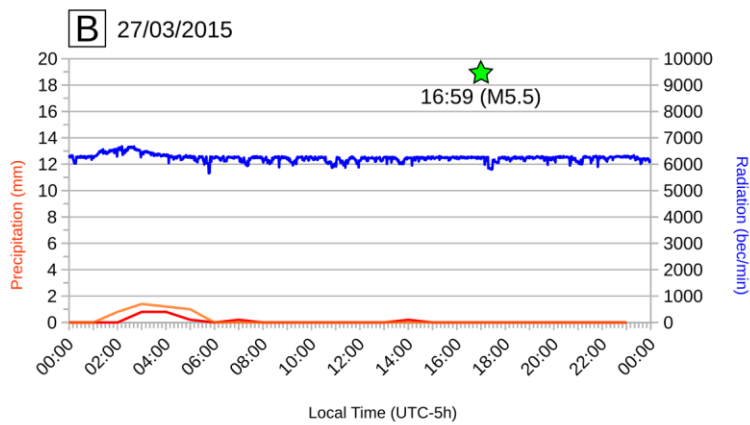
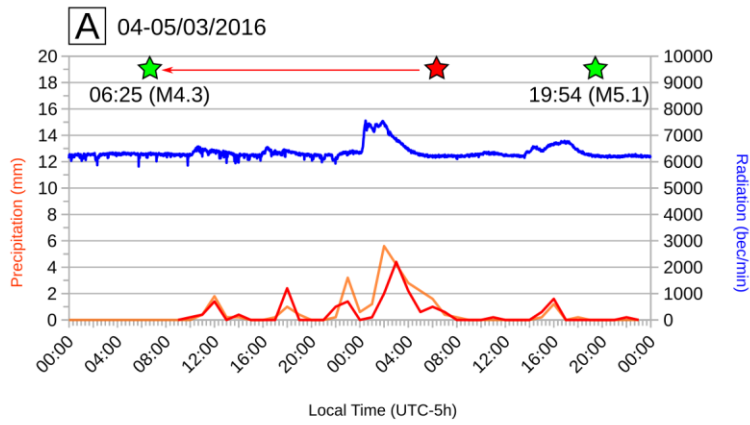


Figure C1. Examples showing relationship between rainfalls occurrence and radiation level measured in Lasso. A: corresponds to Figure 4B in Toulkeridis et al. (2019). Their Figure 4B misplaced the M 4.3 earthquake by approximately one day. The real span between the M 4.3 and M 5.1 earthquakes is 37 hours 29 minutes. Radiation time series are also offset by ~24 hours when taking into account the date on the Figure 4B from Toulkeridis et al. (2019). B: example of an earthquake without radiation anomaly within 6 hours before the occurrence. C: example of a radiation anomaly with its corresponding precipitation peak and no earthquake. D: M 7.8 earthquake on 16<sup>th</sup> April 2016, with a clear precipitation peak at the time of the radiation anomaly. M 5.5 earthquake not shown in Toulkeridis et al. (2019). Orange line: Vivero weather station; red line: Colcas weather station, blue line: NOVACERO radiation detection; green star: earthquakes with time and magnitude from the NEIC catalog (<https://earthquake.usgs.gov/earthquakes/search/>); red star: wrongly located earthquake in Toulkeridis et al. (2019).

121 According to our results, the alarm rate (number of anomalies divided by the duration of the time  
122 series, which is 462 days, ~15 months) is 10.8 alarms per month, with a success rate (number of  
123 anomalies detected prior to the earthquakes divided by the total number of anomalies) of 2.5%.  
124 Furthermore, the association level between earthquakes and anomalies (number of earthquakes  
125 preceded by a radiation anomaly divided by the total number of earthquakes) is 21%. In other words,  
126 the method proposed by Toulkeridis et al. (2019) would have emitted one valid alarm out of every  
127 five earthquakes, with  $M \geq 5$ , and would have provided 40 false alarms for every true earthquake  
128 during the studied period. Based on our statistical analysis, we refute the authors statement that their  
129 method allows to predict earthquakes or to issue medium term forecasts. Furthermore, we observe  
130 that the authors chose to present only the few earthquakes that support their claim. They sloppily  
131 use earthquakes with magnitudes  $M < 5$ , and shifted in time an earthquake in their Figure 4B so that  
132 it supports their claim.

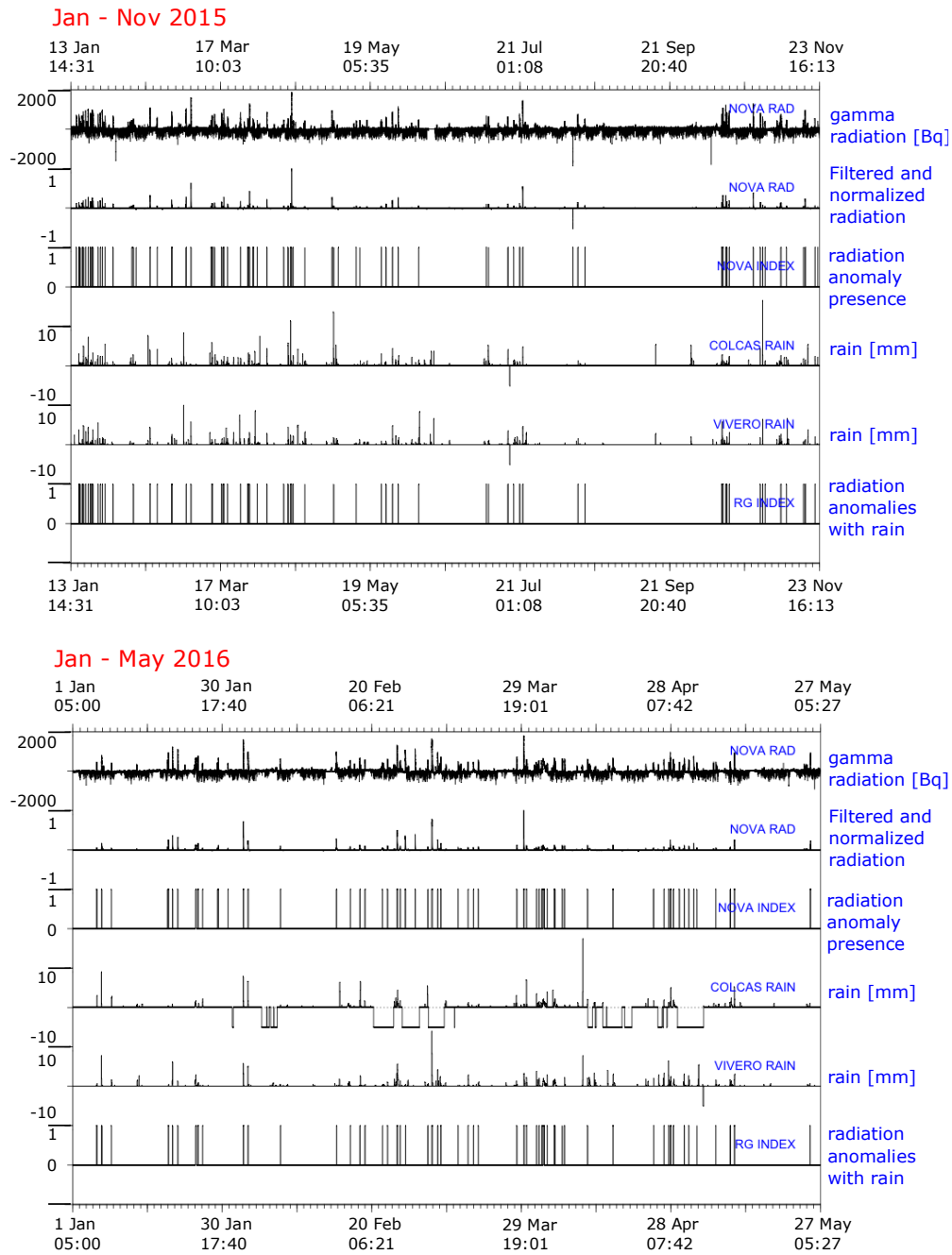
133 Considering the high alarm rate, the large percentage of false alarms, and the low association level  
134 between earthquakes and radiation anomalies, the methodology presented by Toulkeridis et al.  
135 (2019) does not provide a valid operational earthquake precursor detector. In the next section we  
136 explore a different source for the gamma radiation anomalies.

### 137 2.3. Counter-hypothesis: atmospheric anomalies

138 Toulkeridis et al. (2019) consider that “anomalies may occur due to a variety of natural or artificial  
139 effects, such as strong rainstorms” but in their analysis they fail to present any early procedure to  
140 distinguish storm-related gamma rays (Suszcynsky et al., 1996, Marisaldi et al., 2013) from those  
141 related to earthquakes. According to the instrument manual user, the background radiation level is  
142 constantly changing due to cosmic events, weather and other influences (LUDLUM, 2014). In  
143 particular, the operator’s manual clearly states that “changes in background radiation due  
144 (especially) to precipitation can increase the radiation level seen by the detector by 300%”. We  
145 therefore assess the impact of rainfall on the radiation time series.

146 We collected hourly rain precipitation data from two rain gauges, Vivero (Lat.: S 0.6947°, Long.: W  
147 78.5887°) and Colcas (Lat.: S 0.7013°, Long.: W 78.5351°), operated by Aglomerados Cotopaxi  
148 S.A. located respectively at 11 and 13 km N-NE from the NOVACERO sensor where no rain gauge  
149 is installed. To compare the gamma radiation and precipitation time series, we interpolate the hourly  
150 rain data to minutes, so that every minute within an hour has the same hourly value. In addition,  
151 gaps are filled with a negative value, and only positive precipitation values are then used in  
152 subsequent analysis. In order to compare the precipitation and the radiation anomalies, we compute  
153 all radiation anomalies (NOVA INDEX in Figure C2) occurring during rainfall periods (RG INDEX  
154 in Figure C2). Both sequences are highly similar, and 138 of the 162 radiation alarms (85%)  
155 correlates with local rains (Figures C1 and C2). The found correlation between rainfalls and  
156 radiation anomalies includes all the alarms interpreted as earthquake precursors by Toulkeridis et al.  
157 (2019) in their Figure 4, and includes the 16<sup>th</sup> April 2016 earthquake (Figure C1). The 24 remaining  
158 alarms could not be associated with the precipitation time series, perhaps because of more localized  
159 rainfalls occurring at Lasso and not recorded by the two rain gauges, or because of other  
160 atmospheric or cosmic processes. However, none of them correlate with  $M \geq 5$  earthquakes within  
161 the specified time windows. From our radiation analysis, we conclude that most radiation  
162 background anomalies at the RPM correlate with local rainfalls. The occurrence of an earthquake  
163 within a 250 km radius from the RPM could easily coincide with the frequent rainfalls in the area.

## Gamma radiation and rain precipitation



164

Figure C2. Gamma radiation and rain precipitation time series and statistical analysis. Top (Jan – Nov 2015) and bottom (Jan – May 2016) panels include the following time series, from top to bottom at each panel. Trace 1: Gamma radiation after its trend is removed (NOVA RAD). Trace 2: Filtered gamma radiation for periods larger than one hour. Trace 3: One-zero index detecting radiation anomalies (NOVA INDEX). Trace 4: rain precipitation in COLCAS weather station. Trace 5: rain precipitation in VIVERO weather station. Trace 6: One-zero index to simultaneously select those radiation anomalies that occur during rain periods (RG INDEX).

### 165 3. GPS data

166 Toulkeridis et al. (2019) show GPS 1-sample-per second kinematic analysis result for sites located  
167 from a few tens to a few hundreds of kilometers from the rupture area. Summarized in their Figure  
168 7, the general behavior of the calculated positions is: (1) a random apparent displacement confined  
169 within a ~1 m wide ellipse during the hours before the M 7.8 earthquake; (2) a westward to  
170 southwestward transient motion of several tens of centimeters, exceeding a meter at a few sites  
171 during “several minutes prior the main earthquake event”; (3) a sudden northward jump, taking  
172 place during a single second and at the same second at all sites. This displacement is similar in  
173 direction at all sites and exceeds one meter in magnitude for more than half of the sites, including  
174 sites located at ~200 km (CHEC) or even ~300 km (FOEC) from the rupture area; (4) a random  
175 displacement within ~60 cm during the seconds following the jump.

#### 176 3.1. GPS co-seismic offsets

177 The displacements during the earthquake proposed by Toulkeridis et al. (2019) are physically  
178 impossible. This is because if two GPS stations record the jump at the same second but are located  
179 at a different distance from the source, as presented in Toulkeridis et al. (2019), then the seismic  
180 waves must have travelled at a velocity faster than the difference of their distance from the  
181 epicenter during less than a second. Taking for instance, ONEC (long. W 80.10°, lat. S 0.70°, 50 km  
182 from the epicenter) and FOEC (long. W 76.99°, lat.S 0.46°, 300 km from the epicenter), would give  
183 a seismic velocity larger than 250 km/s, that is roughly two orders of magnitude faster than known  
184 P-wave velocity traveling the lithosphere. Movement of more than 1 m in a second would imply a  
185 very large acceleration that would have resulted in significant damages all over Ecuador which is at  
186 odd with the report of damages and observation from the accelerometric network (Beauval et al.,  
187 2017). Third, the offsets reported by Toulkeridis et al. (2019) is northward for all sites, regardless  
188 their location with respect to the rupture area. NJEC (long. W 79.62°, lat. S 2.67°), CHEC (long. W  
189 77.81°, lat. S 0.34°) or FOEC (long. W 76.99°, lat.S 0.46°), all located more than 200 km from the

190 rupture, show larger displacements than ONEC (long. W 80.10°, lat. S 0.70°) located ~50 km from  
191 the rupture. These results are inconsistent with the prediction of elastic models for a slip on the  
192 megathrust, that should mainly induce trenchward displacements with magnitude of displacement  
193 decreasing with increasing distance from the slip area.

194 Moreover, the offsets reported by Toulkeridis et al. (2019) are inconsistent with previously reported  
195 offset for the same sites from kinematic analysis (Nocquet et al., 2017) and co-seismic offsets  
196 derived from a regional static analysis of GPS data (Nocquet et al., 2017, Mothes et al., 2018).  
197 Static offsets can also be estimated from the high-rate GPS kinematic analysis presented in Ruhl et  
198 al. (2018) (freely available at <https://zenodo.org/record/1434374>). Ruhl et al. (2018), Nocquet et al.  
199 (2017) and Mothes et al. (2018) results consistently show a maximum static offset of 75 cm and 50  
200 cm on the horizontal and vertical components respectively near the rupture area, rapidly decreasing  
201 to less than 7 cm and 2 cm at QVEC (95% confidence level). The static co-seismic displacement at  
202 QVEC (long. W 79.47°, lat. S 1.01°) can be independently assessed from InSAR results published  
203 using Sentinel-1 and ALOS ascending and descending tracks (He et al., 2017, Nocquet et al., 2017,  
204 Gombert et al., 2017, Yi et al., 2018). For all results, the InSAR data indicate less than 10 cm of co-  
205 seismic displacement in the satellite line-of-site, consistent with GPS estimates. The estimates from  
206 Toulkeridis et al. (2019) are therefore ~20 to 35 times larger than all other InSAR and GPS  
207 estimates.

208 High-Rate GPS kinematic analysis of Ecuador GPS sites recorded the seismic waves induced by the  
209 Pedernales earthquake (Nocquet et al., 2017, Ruhl et al., 2018) and are further consistent with  
210 kinematic modelling of the rupture propagation (Nocquet et al., 2017, Gombert et al., 2018) or with  
211 the Peak Ground Displacement-Moment Magnitude scaling relationship (Ruhl et al., 2018).  
212 Magnitude and timing of onset of the seismic waves differs among stations as a function of their  
213 location with respect to the evolving slip during the rupture as expected from elasto-dynamic

214 solutions. Toulkeridis et al. (2019) results are inconsistent with the known physics of earthquakes  
215 and seismic waves propagation.

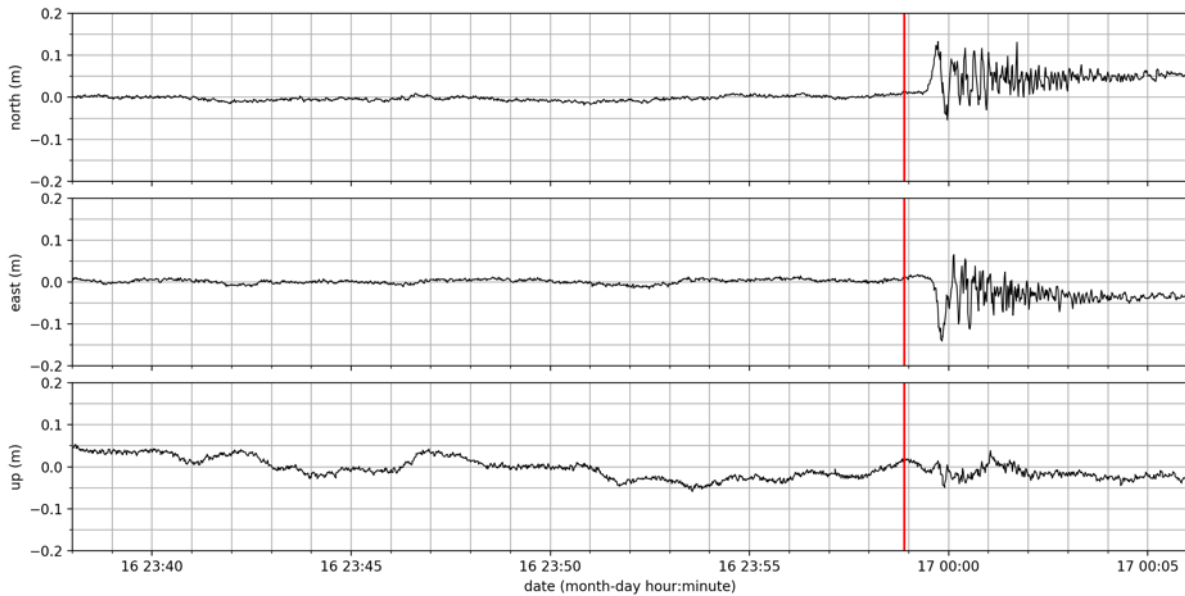
### 216 3.2. Kinematic analysis of QVEC data

217 Proper kinematic analysis of high-rate GPS data including phase measurements typically show  
218 precision of a few centimeters or less (e.g. Genrich and Bock, 2006). Toulkeridis et al. (2019)  
219 results prior the M 7.8 Ecuador earthquake show a dispersion of the order of 1 meter or more (their  
220 Figure 5 & 7), that is 50 times larger than state-of-the-art kinematic analysis. We present our own  
221 processing of the same data as Toulkeridis et al. (2019) for the QVEC site focusing on a time  
222 window starting ~20 minutes before the earthquake. The red line in Figure C3 corresponds to the  
223 time origin of the earthquake provided by the USGS at 23:58:36 UTC. We translate this time into  
224 GPS time so that our figure can be readily compared with figure 5B from Toulkeridis et al. (2019)  
225 as they do not mention the GPS time-UTC correction. With respect to Toulkeridis et al. (2019), our  
226 processing shows the following differences: (1) the first peak displacement develops during almost  
227 20 seconds and not during a single second; (2) the maximum amplitude is less than 15 cm for all  
228 components and not 1 meter; (3) the east component records significant displacement; (4) the static  
229 displacement seen at the end of the signal is -4 cm, +5 cm, -2.5 cm on the east, north and up  
230 components respectively in agreement at the centimeter level with the values published in Nocquet  
231 et al. (2017) and Mothes et al. (2018).

232 On the contrary to Toulkeridis et al. (2019), our processing shows a stability with no departure  
233 larger than 2 cm from the mean for the horizontal components (standard deviation 0.5 and 0.6 cm  
234 for the north and east components respectively). The vertical component is noisier as expected with  
235 a standard deviation of 3.0 cm.

236 As a consequence, a processing which shows a low noise compared to Toulkeridis et al. (2019)  
237 GPS results, provides results consistent with the timing and amplitude of the seismic waves and

238 static offset does not see any evidence of abnormal transient motion during the minutes preceding  
239 the Pedernales earthquake. Centimeter level fluctuations rather reflect changing geometry of the  
240 satellite, mismodelling of tropospheric delays, but certainly not “normal displacement” as written in  
241 Toulkeridis et al. (2019). Our processing rules out any displacement larger than 2 cm and  
242 definitively excludes the one-meter precursory motion proposed by Toulkeridis et al. (2019).



243

Figure C3: 1-sample-per-second kinematic analysis of QVEC site GPS data. The red line indicates the origin time of the M M 7.8 Pedernales earthquake on April 16<sup>th</sup> 2016 (23:58:36 UTC) in GPS time (23:58:53).

244

#### 245 4. Conclusion

246 Both analyses of radiation and GPS time series from Toulkeridis et al. (2019) show major flaws. We  
247 demonstrate that radiation anomalies are seen only for the three earthquakes shown in Toulkeridis et  
248 al. (2019) over a set of 19  $M \geq 5$  earthquakes, while a total of 162 radiation anomalies occurred  
249 during the 15-month period of analysis. Therefore, their hypothesis that radiation anomalies are  
250 reliable earthquake precursors has to be rejected. We also show that radiation anomalies and  
251 rainfalls recorded near the sensor show a high time correlation. Research is required to explore the

252 triggering mechanisms for radiation anomalies, before any further use. There is no obvious ground  
253 displacement during the minutes preceding the Pedernales earthquake and Toulkeridis et al. (2019)  
254 results about the displacement during the earthquake are unrealistic. As a consequence, we conclude  
255 that the earthquake prediction methodology and the early warning system proposed by Toulkeridis  
256 et al. (2019) are unfounded.

257 Earthquake prediction/forecast science has made sustained progress in the last decades, but the  
258 unique determination of the location, time and magnitude of a specific earthquake beforehand still  
259 remains elusive (Jordan et al. 2011). A variety of proposed precursors –seismic, geodetic,  
260 electromagnetic, geochemical, radiation– do not yet provide the diagnostic capability needed for  
261 operational predictions because the signal behavior in the absence of earthquakes is often not  
262 characterized (REMAKE, 2016). Nevertheless, the study of earthquake precursors should not be  
263 abandoned. Negative results are also important elements of scientific progress (Nature Editor, 2017),  
264 but research cannot self-correct when information is missing. Therefore, we suggest that all the data  
265 presented in Toulkeridis et al. (2019) should be openly accessible so that any scientist can evaluate  
266 them. Independent and rigorous assessment of precursors is particularly important if public  
267 authorities are to be able to use scientific results confidently to define earthquake prevention and  
268 preparedness policies, and the scientific community as a whole must ensure that this confidence is  
269 maintained.

270

## 271 **Acknowledgment**

272 We thank an anonymous reviewer that helped us to improve the present comment. Gamma radiation  
273 data were provided by NOVACERO and rain precipitation data by Aglomerados Cotopaxi S.A.,  
274 with a special acknowledgment to María Gallardo and Roberto Neumann.

275

276 **References**

- 277 Beauval C, Marinière J, Laurendeau A, Singaicho J-C, Viracucha C, Vallée M, Maufroy E,  
278 Mercerat D, Yepes H, Ruiz M, Alvarado A (2017) Comparison of Observed Ground-Motion  
279 Attenuation for the 16 April 2016 M 7.8 Ecuador Megathrust Earthquake and Its Two Largest  
280 Aftershocks with Existing Ground-Motion Prediction Equations. *Seismological Research Letters*  
281 88:287–299. doi: 10.1785/0220160150
- 282 Chen YI, Liu JY, Tsai YB, Chen CS (2004) Statistical tests for pre-earthquake ionospheric anomaly.  
283 *Terrestrial, Atmospheric and Oceanic Sciences* 15, 385–396.
- 284 Geller RJ (1997) Earthquake prediction: a critical review. *Geophysical Journal International*, 131,  
285 425–450. doi: 10.1111/j.1365-246X.1997.tb06588.x
- 286 Genrich JF, Bock Y (2006) Instantaneous geodetic positioning with 10–50 Hz GPS measurements:  
287 Noise characteristics and implications for monitoring networks. *Journal of Geophysical Research:*  
288 *Solid Earth*, 111(B3). doi: 10.1029/2005JB003617
- 289 Gombert B, Duputel Z, Jolivet R, Simons M, Jiang J, Liang C, Fielding EJ, Rivera L (2018) Strain  
290 budget of the Ecuador–Colombia subduction zone: A stochastic view. *Earth and Planetary Science*  
291 *Letters* 498:288–299. doi: 10.1016/j.epsl.2018.06.046
- 292 He P, Hetland EA, Wang Q, Ding K, Wen Y, Zou R (2017) Coseismic slip in the 2016 Mw 7.8  
293 Ecuador earthquake imaged from Sentinel-1A radar interferometry. *Seismological Research Letters*,  
294 88(2A), 277-286. doi: 10.1785/0220160151
- 295 Jordan TH, Chen Y-T, Gasparini P, Madariaga R, Main I, Marzocchi W, Papadopoulos G, Sobolev G,  
296 Yamaoka K, Zschau J (2011) Operational Earthquake Forecasting. State of Knowledge and  
297 Guidelines for Utilization. *Annals of Geophysics* 54. doi: 10.4401/ag-5350

298 Kolbert, E. (2015). The Shaky Science Behind Predicting Earthquakes. *Smithsonian Magazine*,  
299 [https://www.smithsonianmag.com/science-nature/shaky-science-behind-predicting-earthquakes-](https://www.smithsonianmag.com/science-nature/shaky-science-behind-predicting-earthquakes-180955296/)  
300 180955296/

301 LUDLUM (2014) LUDLUM model 4525 series radiation portal monitor operator's manual. Version  
302 3.4.0 / 39653N01.

303 Marisaldi M, Fuschino F, Labanti C, Tavani M, Argan A, Del Monte E, Longo F, Barbiellini G,  
304 Giuliani A, Trois A, Bulgarelli A, Gianotti F, Trifoglio M, 2013. Terrestrial Gamma-Ray Flashes,  
305 *Physics Research A*, 720, 83-87. doi: 10.1016/j.nima.2012.12.019.

306 Mothes PA, Rolandone F, Nocquet J-M, Jarrin PA, Alvarado AP, Ruiz MC, Cisneros D, Páez HM,  
307 Segovia M (2018) Monitoring the Earthquake Cycle in the Northern Andes from the Ecuadorian  
308 cGPS Network. *Seismological Research Letters* 89:534–541. doi: 10.1785/0220170243

309 National Research Council (2003). *Living on an Active Earth: Perspectives on Earthquake Science*.  
310 Washington, DC: The National Academies Press. doi: 10.17226/10493

311 Nature editor (2017) Nurture Negatives. *Nature*, 551, 414, doi: 10.1038/d41586-017-07325-2

312 Nocquet J-M, Jarrin P, Vallée M, Mothes PA, Grandin R, Rolandone F, Delouis B, Yepes H, Font Y,  
313 Fuentes D, Régnier M, Laurendeau A, Cisneros D, Hernandez S, Sladen A, Singaicho J-C, Mora H,  
314 Gomez J, Montes L, Charvis P (2017) Supercycle at the Ecuadorian subduction zone revealed after  
315 the 2016 Pedernales earthquake. *Nature Geoscience* 10:145–149. doi: 10.1038/ngeo2864

316 REMAKE: Seismic Risk in Ecuador: Mitigation, Anticipation and Knowledge of Earthquakes  
317 (2016), ANR (ANR-15-CE04-0004) (2016). <https://remake.osug.fr/?lang=fr>

318 Ruhl, C. J., Melgar, D., Geng, J., Goldberg, D. E., Crowell, B. W., Allen, R. M., ... & Cabral-Cano,  
319 E. (2018). A Global Database of Strong-Motion Displacement GNSS Recordings and an Example  
320 Application to PGD Scaling. *Seismological Research Letters*, 90(1), 271-279. doi:  
321 10.1785/0220180177

- 322 Suszcynsky DM, Roussel-Dupre R, Shaw G (1996) Ground-based search for X rays generated by  
323 thunderstorms and lightning. *Journal of Geophysical Research: Atmospheres* 101:23505–23516. doi:  
324 10.1029/96JD02134
- 325 Toulkeridis T, Porras L, Tierra A, Toulkeridis-Estrella K, Cisneros D, Luna M, Carrión JL, Herrera  
326 M, Murillo A, Perez Salinas JC, Tapia S, Fuertes W, Salazar R (2019) Two independent real-time  
327 precursors of the 7.8 M earthquake in Ecuador based on radioactive and geodetic processes –  
328 Powerful tools for an early warning system. *Journal of Geodynamics*, accepted. doi:  
329 10.1016/j.jog.2019.03.003
- 330 Uyeda S, Nagao T, Kamogawa M (2009) Short-term earthquake prediction: Current status of  
331 seismo-electromagnetics. *Tectonophysics* 470:205–213. doi: 10.1016/j.tecto.2008.07.019
- 332 Yi L, Xu C, Wen Y, Zhang X, Jiang G (2018) Rupture process of the 2016 M 7.8 Ecuador  
333 earthquake from joint inversion of InSAR data and teleseismic P waveforms. *Tectonophysics*, 722,  
334 163-174. doi: 10.1016/j.tecto.2017.10.028